Pergamon

0890-4332(94)00082-4

A NEW INSTRUMENT FOR RADIATION HEAT FLUX MEASUREMENT—ANALYSIS AND PARAMETER SELECTION

N. Martins, M. G. Carvalho, N. H. Afgan* and A. I. Leontiev†

Instituto Superior Técnico, Dept Eng. Mecânica, 1º. Piso Pav. Máquinas, 1096 Lisbon, Portugal; and
†Moscow Technical University, Moscow, Russia

Abstract—In a number of combustion chambers, differentiation between radiation and convective heat transfer on the surface is a problem of substantial interest. The hemispherical radiation heat flux meter proposed by Afgan and Leontiev [1] and patented by Afgan, Carvalho, Martins and Leontiev [2] has potential to be used as an instrument with sufficient accuracy to measure the difference between hemispherical radiation heat flux and convective heat flux in the respective environments.

The hemispherical radiation flux meter is numerically analyzed with the aim of defining the optimal design parameters to be used for experimental verification. With a proper selection of the design parameters corresponding to the conditions encountered in the boiler furnace, it will be possible to measure with the same instrument the radiation heat flux and convective heat flux.

Particular attention was focused on the discussion of the respective parameters of the flux meter in order to meet corresponding requirements in different environments. Attention was focused on the effects of differences in main mass flow rate and blow-off gas mass flow rate, heat conductivity of the holder and porous filament and the difference in temperature between solid structure and fluid flow in the filament.

For the selected parameters of the main flow and radiation heat flux range, the radiation heat flux meter was designed.

NOMENCLATURE

A_0 specific surface area
C blow-off constant
C_p Specific heat
D diameter
h convection heat transfer coefficient
J blow-off mass flow rate
K permeability
k thermal conductivity
L thickness
n number of pores
Nu Nusselt number
p pressure
Pr Prandtl number
Q heat flux
r radial direction coordinate
Re Reynolds number
S source term
T temperature
u velocity
x axial direction coordinate
y transversal coordinate

Greek letters

Δ difference
ϵ porosity
μ viscosity
π 3.1415....
ρ density

---

*Author to whom correspondence should be addressed.

1. INTRODUCTION

Thermal radiation measurement is an important parameter for the diagnosis of a number of systems. Boilers, furnaces and combustion chambers are among those systems, where the most important parameter to be determined is the thermal radiation flux at the respective walls. A number of attempts have been made to develop an instrument for heat flux measurement in the enclosures [3–6].

With varying success, most of the methods have been used in the control and diagnostics of the systems. There are different limitations observed for each of the specific instrument designs. For this reason, the development of the new heat flux measurement method is a challenging incentive. In particular, the thermal radiation flux measurement in a hostile environment is needed to meet the requirement of the respective diagnostic of the system.

The new instrument for the thermal hemispherical radiation flux measurement [1], is based on the determination of the temperature difference of the gas flowing through the porous filament exposed to the respective heat flux to be measured (Fig. 1). When the critical blow-off gas mass flow rate is reached the boundary layer is blown-off from the porous surface exposed to the hot
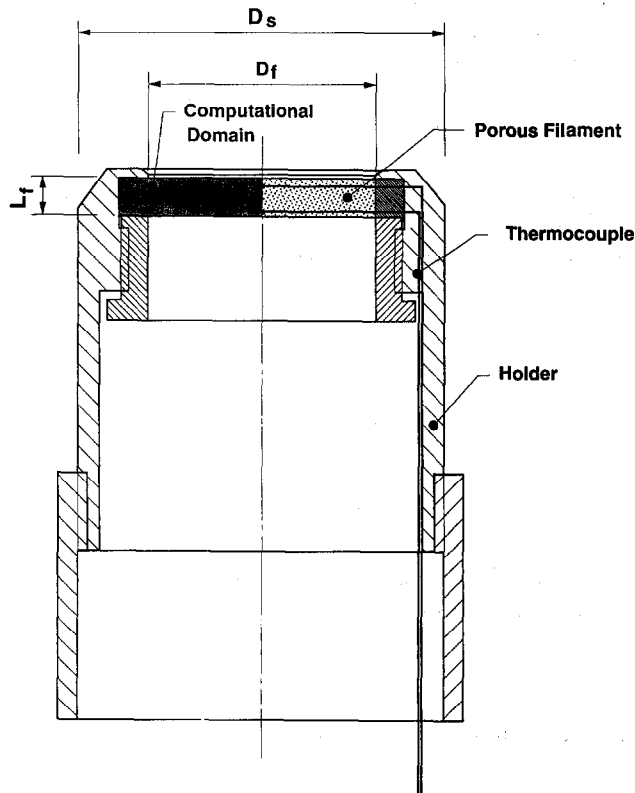

Fig. 1. The flux meter head.

gas environment. Heat transfer and fluid flow in the porous filament have to be respectively selected, in order to meet requirements posed by the instrument to reach corresponding accuracy and material limitations.

For this reason, this study is devoted to the numerical analysis of the parameters affecting the imposed limitations of the instrument. In this respect, special attention is devoted to the analysis of the global parameters of the instrument and also to the analysis of the gas velocity and temperature distribution in the porous filament. In order to determine physical dimensions, gas and porous material parameters analysis is focused on the specific limitations imposed by the hostile environment where the instrument is supposed to work. The selection of the geometrical and physical parameters of the instrument is based on the analysis of the presented numerical study of the problem.

2. MATHEMATICAL MODEL

2.1. Introduction

To assist the development of the heat flux sensor, two mathematical models were implemented. The first model is based on integral energy and mass balances, assuming the porous filament as a set of aligned capillary ducts with a laminar air flow through them. This model was used to define the limits within which the most important design parameters should be for a certain set of working conditions.

The second model is based on the numerical solution of the energy, momentum and continuity differential equations in their 2-D-axisymmetric, steady-state form for a homogeneous porous media crossed by a laminar air flow. Local thermal equilibrium between gas and solid phases is not valid so the model considers separated energy equations for each present phase coupled by a source term.

2.2. Critical blow-off gas mass flow rate

The critical blow-off gas mass flow rate required to promote the destruction of the boundary layer over the porous filament is a basic parameter to be defined for this heat flux sensor.

Under the influence of the blow-off gas on the boundary layer at the vicinity of the wall, a momentum transfer from the blow-off gas to the main stream will take place, leading to the decrease of the main stream gas velocity in the vicinity of the wall, this will result in a decrease of the velocity gradient $(\partial u/\partial y)_w$. As a consequence of the velocity profile deformation and an increase of the boundary layer thickness, a decrease of the friction force is obtained under other constant conditions. With the increase of the blow-off gas mass flow rate, the velocity profile on the boundary layer will present an inflection point characterized by $(\partial u/\partial y)_w = 0$. In the definition of this point, the critical blow-off gas mass flow rate is introduced by Leontiev [7] as

$$J_{cr} = C \frac{\rho_0 u_0}{\sqrt{Re_0}} \tag{1}$$

$$Re_0 = \frac{\rho_0 U_0 D}{\mu_0}, \tag{2}$$

where C is a constant dependent on the geometry.

These equations relate the gas mass flux through the porous filament with the conditions at the vicinity of its wall surface.

Figure 2 shows the critical blow-off gas mass flow rate for different porous filament diameters, as a function of the external flow velocity, considering $C = 0.62$ and assuming a main stream flow temperature of 1200 K.

2.3. Integral balance model

A simple model based on integral balances of energy and mass and considering the porous filament as a set of capillary ducts was developed. The model considers a Darcean laminar flow through the ducts and constant fluid properties. Due to its importance, the critical blow-off mass flow rate range was considered (from the *blowing-off* point of view). The studied parameters are:
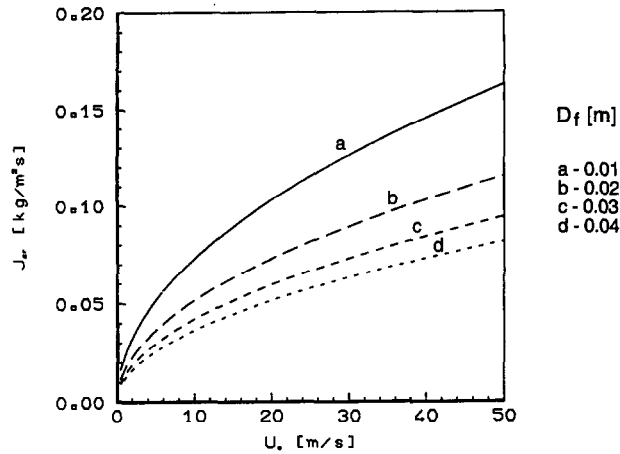
Fig. 2. Critical blow-off gas flow rate for an infinite slab.

—temperature difference of the air flow between the inlet and outlet surfaces of the porous filament,

—pressure drop in the porous filament,

—temperature difference between gas and solid phases.

The integral energy balance assumes that all the energy received by a filament is transferred to the fluid and that the lateral walls of the filament are adiabatic. The temperature difference of the gas between inlet and outlet surfaces is given by

$$\Delta T = \frac{Q}{c_p J} \tag{3}$$

The pressure drop through the porous filament for a laminar, fully-developed flow in a duct was considered, and the Hagen–Poiseuille equation was used in the form of a Darcy law as a function of the mass flow rate as follows:

$$\Delta p = \frac{32 \, \mu_g L_f}{\epsilon D_p^2 \rho_g} J \tag{4}$$

The temperature difference between the gas and solid phases was determined under the same assumption of the previous paragraph, i.e. considering a Hagen–Poiseuille flow inside each pore. The heat flux received by the porous skeleton is transferred to the gas by convection, so that

$$\Delta T_{\ln} = \frac{Q}{n\pi k_g L_f N u}, \tag{5}$$

where the Nusselt number is determined by correlations valid for laminar forced convection through cylindrical tubes.

2.4. Differential balance model

A more detailed mathematical model of the heat and mass transfer in a porous media crossed by an air flow was developed. The model is based on the solution of the differential conservation equations for energy in each phase, in addition to the momentum and continuity equations in the gas phase. The equations are considered in their two-dimensional, steady-state form and are solved in cylindrical coordinates by a finite difference (control volume) technique. The set of equations constituting the mathematical model is as follows:

Continuity

$$\frac{\partial}{\partial x}(\rho u_x) + \frac{1}{r}\frac{\partial}{\partial r}(r\rho u_r) = 0 \tag{6}$$

Momentum

$$\rho u_x \frac{\partial u_x}{\partial x} + \rho u_r \frac{\partial u_x}{\partial r} + \frac{\partial p}{\partial x} - \frac{\partial}{\partial x} \left(\mu \frac{\partial u_x}{\partial x} \right) - \frac{1}{r} \frac{\partial}{\partial r} \left(\mu r \frac{\partial u_x}{\partial r} \right) - S_x = 0 \qquad (7)$$

$$\rho u_x \frac{\partial u_r}{\partial x} + \rho u_r \frac{\partial u_r}{\partial r} + \frac{\partial p}{\partial r} - \frac{\partial}{\partial x} \left(\mu \frac{\partial u_r}{\partial x} \right) - \frac{\partial}{\partial r} \left(\mu \frac{1}{r} \frac{\partial}{\partial r} (ru_r) \right) - S_r = 0 \qquad (8)$$

Energy (gas)

$$\rho u_x \frac{\partial h}{\partial x} + \rho u_r \frac{\partial h}{\partial r} - \frac{\partial}{\partial x} \left(\frac{\mu}{Pr} \frac{\partial h}{\partial x} \right) - \frac{1}{r} \frac{\partial}{\partial r} \left(\frac{\mu}{Pr} r \frac{\partial h}{\partial r} \right) - S_h = 0 \qquad (9)$$

Energy (solid)

$$\frac{\partial}{\partial x} \left(k_{eff} \frac{\partial T_s}{\partial x} \right) + \frac{1}{r} \frac{\partial}{\partial r} \left(k_{eff} r \frac{\partial T_s}{\partial r} \right) + S_h = 0 \qquad (10)$$

Momentum equation source terms, S_x, S_r. An additional source term appears on the momentum equation because the porous structure is treated as continuous. Several attempts are being made in order to arrive at an equation equivalent to the Navier–Stokes equation, for the description of fluid flow through porous media [8]. A *semiheuristic volume-averaged* treatment of the flow field was made by adding a source term with two components to the standard momentum equations. The first component accounts for the microscopic shear stress (Darcy term) the second component describes the microscopic inertial force (Ergun inertial term):

$$S_i = \frac{\mu}{K} u_i + \frac{1.8 (1 - \epsilon)}{D_p \epsilon^3} \rho u_i^2 \quad (i = x, r), \qquad (11)$$

where

$$K = \frac{\epsilon^3 D_p^2}{180 (1 - \epsilon)^2} \qquad (12)$$

Energy equation source term, S_h. The coupling of the solid matrix and the gas flow energy equation is made through a source term representing the energy transfer between the phases,

$$S_h = A_{spc} h_{sg} (T_s - T_g) \qquad (13)$$

The interstitial convection heat transfer coefficient used, h_{sg}, was experimentally evaluated by Wakao and Kaguey for packed beds for spherical particles [9]. The simple cubic arrangement geometry was considered to determine the specific surface area, A_{spc}.

$$A_{spc} = \frac{\pi}{D_p} \qquad (14)$$

$$h_{sg} = \frac{k_g}{d_p} (2 + 1.1 \, Re^{0.6} Pr^{1/3}) \qquad (15)$$

Effective thermal conductivity, K_{eff}. A considerable review of the many available studies for the determination of K_{eff} can be found in reference [8]. In this study, as a first approach, a geometric mean (between gas and solid thermal conductivity) was considered.

$$k_{eff} = k_g^\epsilon \cdot k_s^{(1-\epsilon)} \qquad (16)$$

Boundary conditions. The assumed boundary conditions are listed in Table 1.

2.5. Numerical procedure

Method of solution. In the present work, a finite difference approach was used to solve the equations of the model described above. The hybrid central/upwind method was used to discretize the convection terms [10] and the pressure coupling was performed with the SIMPLE algorithm [11]. After each iteration, the thermo–physical properties of solid and gas phases are updated, as well as the source terms of the energy and momentum equations.

Table 1. Boundary conditions

	$x = 0.0$	$x = L$	$r = 0.0$	$r = R_1$
Continuity	$u_r = 0.0$	$u_r = 0.0$	$u_r = 0.0$	$u_r = 0.0$
	$u_x = \dfrac{j}{\rho}$	$\dfrac{\partial u_x}{\partial x} = 0.0$	$u_x = 0.0$	$u_x = 0.0$
x Momentum	$u_x = \dfrac{j}{\rho}$	$\dfrac{\partial u_x}{\partial x} = 0.0$	$\dfrac{\partial u_x}{\partial r} = 0.0$	$u_x = 0.0$
r Momentum	$u_r = 0$	$u_r = 0$	$\dfrac{\partial u_r}{\partial r} = 0.0$	$u_r = 0.0$
Energy (gas)	$T_g = T_g^i$	$\dfrac{\partial T_g}{\partial x} = 0.0$	$\dfrac{\partial T_g}{\partial r} = 0.0$	$\dfrac{\partial T_g}{\partial r} = 0.0$
Energy (solid)	$\dfrac{\partial T_s}{\partial x} = 0.0$	$k_{eff}\dfrac{\partial T_s}{\partial r} = Q$	$\dfrac{\partial T_s}{\partial r} = 0.0$	$k_{eff}\dfrac{\partial T_s}{\partial r} = Q$

Some computational details. The presented model was applied to the prediction of the mean flow and heat transfer between the gas and the solid matrix in the instrument *holder.* The *holder* is considered as the part of the instrument where the porous filament is accommodated, as is shown in Fig. 1. The computational domain is represented in Fig. 1, both the porous filament and part of the holder are considered. Due to symmetry reasons, a single slice of the sensor was studied. The thickness of the holder was the same for all the tests made (5.0 mm). A staggered grid with 20 × 20 nodes was used. As a convergence criterion we considered that the dimensionless residual sources of all equations should be smaller than 0.005 and the integral energy balance should be satisfied.

Based on the results of the integral balance model, a first selection of parameters was made, in order to perform a more detailed analysis with the differential balance model. The studied parameters are listed in Table 2.

3. DISCUSSION OF THE RESULTS

The results obtained with the developed models have been used to select the required characteristics of the heat flux meter and to define the range of parameters under which it can meet limitations imposed by its design, working conditions and materials. Attention was also devoted to determine the limitation imposed by the requirement of using the same instrument for radiation heat transfer and convection heat transfer in the hot gas environment.

3.1. *Selection criteria*

The selection of geometric and operating design characteristics for the heat flux meter was based on the following criteria:

Accuracy to be obtained by the instrument. The accuracy of the instrument is defined by the ratio of the temperature distribution in the filament to the uniform temperature, as a measure of the heat loss due to the temperature distribution in the filament.

Physical limitation of the material. For the selected range of working conditions, the filament material may not exceed its temperature limitations. The selected design parameters have to meet these requirements under prescribed conditions.

Table 2. Studied parameters

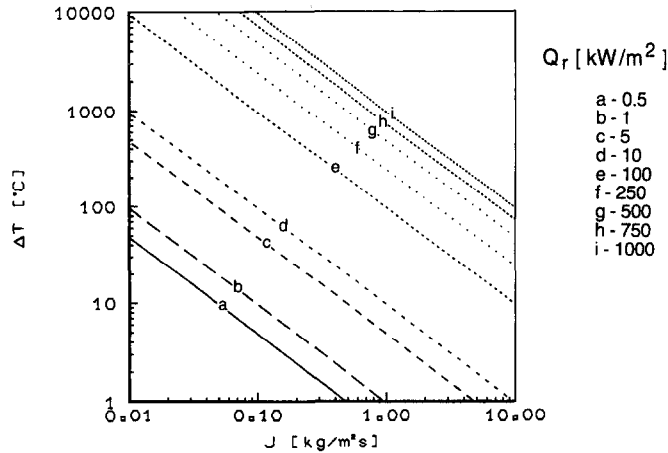| Parameter	Considered values	Units
Blow-off gas mass flow rate, J	2 and 8	$kg\,m^{-2}\,s^{-1}$
Filament diameter, D_f	10, 30 and 40	mm
Filament thickness, L_f	5, 15 and 20	mm
Heat flux, Q	50, 100 and 200	$kW\,m^{-2}$
Material	Stainless steel	—
Porosity, ϵ	0.3 and 0.5	—
Size of the pores, D_p	50 and 100	μm

Fig. 3. Predicted temperature difference between the inlet and outlet of the porous filament.

Pressure drop in the filament. In order to prevent strong effects of the blow-off gas to its surroundings and limit excessive use of the blow-off gas, the pressure constrain is introduced as one of the criteria for the design parameter selection.

3.2. *Selection of the principal characteristics of the porous filament*

For the heat flux levels found in industrial boilers ($> 100 \text{ kW m}^{-2}$) the blow-off gas mass flow rate must be some order of magnitude higher than its critical value, to avoid high temperatures in the porous filament, as shown in Fig. 3. Actually, for the considered porous filament diameters, the critical blow-off gas mass flow rate never exceeds $0.15 \text{ kg m}^{-2} \text{s}^{-1}$ (Fig. 2) but to avoid porous filament temperatures higher than 700 K, the blow-off gas mass flow rate has to be between 1 and $10 \text{ kg m}^{-2} \text{s}^{-1}$.

The pressure drop in the porous filament is not a critical parameter if the porosity is equal to or higher than 0.5, as can be seen in Fig. 4.

The analysis of the results obtained by the differential balance model shows that the heat transfer between the gas phase and the solid matrix is controlled by the specific surface area. The temperature difference between the phases is almost zero in all the domains except near the boundary of the porous matrix and solid holder, where a temperature difference can be found.

It can be shown that the first criterion can be satisfied by two options of porous filament:

Option 1—a small diameter (10 mm), large thickness (< 15 mm) and low porosity (0.3).

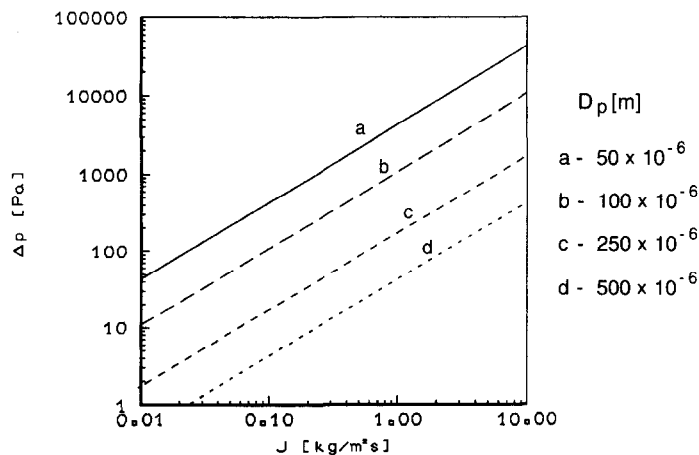*Option* 2—a large diameter (30 mm), small thickness (5 mm) and high porosity (0.5).

Fig. 4. Pressure drop in the porous filament.

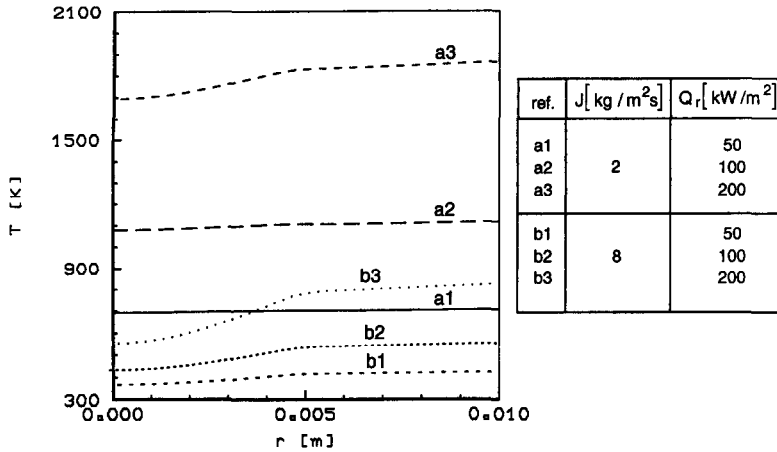| ref.	$J\left[kg/m^2s\right]$	$Q_r\left[kW/m^2\right]$
a1		50
a2	2	100
a3		200
b1		50
b2	8	100
b3		200

Fig. 5. Predicted radial temperature profiles at the porous filament outlet surface (option 1).

With the first option the blow-off gas is heated with a high efficiency, resulting in a very homogeneous temperature distribution on the gas filament. This high heat transfer efficiency is due to the low porosity, large heat exchange surface and high thermal conductivity of the porous matrix. The low porosity is responsible for the high pressure drop.

The second option is characterized by a low heat exchange efficiency between gas and solid phases, mainly due to the high porosity, low thermal conductivity of the porous matrix and small thickness of the filament. As a consequence of the low heat exchange efficiency between the phases, the temperature profile shows a strong influence of the inlet gas temperature that prevails over most of the porous filament surface, with a pronounced change in the vicinity of the boundary between the porous matrix and the solid holder.

Figures 5 and 6 shows radial temperature profiles at the gas outlet for a different heat flux and blow-off gas mass flow rate, respectively, for the first and second solutions.

It may be concluded that the first option may be appropriate for situations where convection heat fluxes must be considered. With a smaller diameter it is easier to reach a critical blow-off gas mass flow rate (Fig. 2), which is essential for this kind of measurement. Due to the low heat fluxes and low blow-off gas mass flow rate, this solution will not present problems with high temperatures and high pressure drops.

The second option is in good accordance with the selection criteria, namely with respect to the required homogeneity of the temperature field in the porous filament, the temperature level (always below 900 K) and the pressure drop (less than 7 kPa for $j = 2\,\mathrm{kg\,m^{-2}\,s^{-1}}$ and 30 kPa for $j = 8\mathrm{kg\,m^{-2}\,s^{-1}}$), for the studied range of blow-off gas mass flow rate, pore diameter and heat flux.

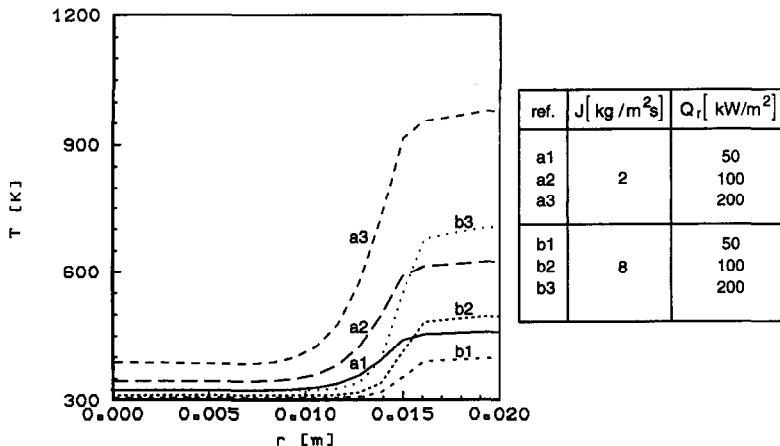The select design parameters for the radiation heat flux meter are given in Table 3.

ref.	$J\left[kg/m^2s\right]$	$Q_r\left[kW/m^2\right]$
a1		50
a2	2	100
a3		200
b1		50
b2	8	100
b3		200

Fig. 6. Predicted radial temperature profiles at the porous filament outlet surface (option 2).

Table 3. Selected design parameters

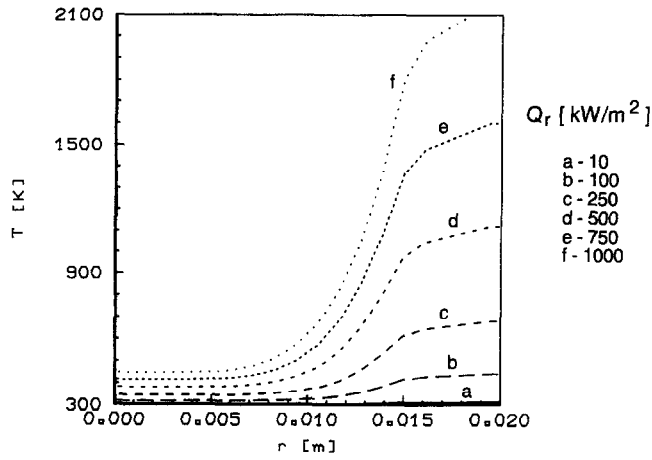| D_f	L_f	D_p	ϵ
30 mm	5 mm	100 μm	0.5

Fig. 7. Predicted radial temperature profiles at the porous filament outlet surface (selected opt.)
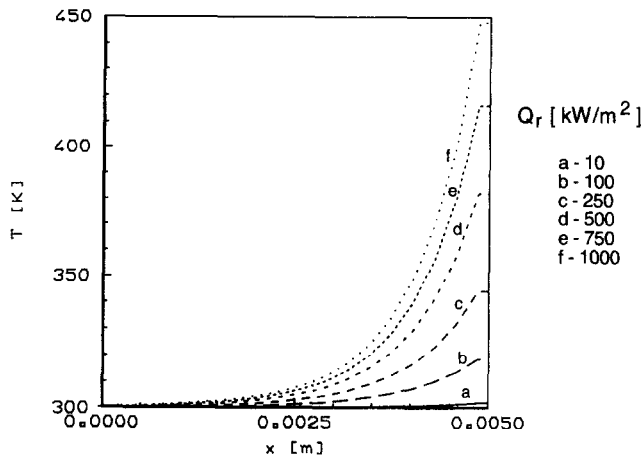

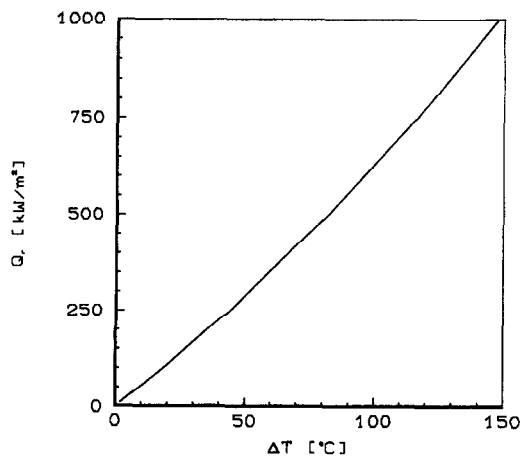Fig. 8. Predicted longitudinal temperature profiles along the porous filament axis (selected opt.).

Fig. 9. Predicted calibration curve for the selected option.

3.3. *Analysis of the selected sensor*

A more detailed analysis of the selected set of design parameters (Table 3) was performed using the differential balance model.

The investigated parameters are the radial and axial temperature profiles (Figs 7 and 8) and the temperature difference between the inlet and outlet surfaces (Fig. 9), for different heat flux levels.

From Fig. 7 it may be concluded that for heat fluxes higher than 500 kW m^{-2} external cooling of the flux meter will be required. Figures 7 and 8 show that for all the heat flux levels considered, there is a core where the influence of the inlet gas temperature is dominant.

It should be stressed that the considered range of heat flux levels covers most of the known engineering applications with high heat fluxes.

Figure 9 shows the predicted calibration curve for the selected porous filament. It shows that the sensor has to be calibrated according to the heat flux levels to be measured, in order to increase its sensitivity. The calibration can be made by adjusting the blow-off gas mass flow rate. The presented curve (Fig. 9) can be used to measure heat fluxes between 250 and 750 kW m^{-2}. For the lower heat fluxes to be considered, the blow-off gas mass flow rate can be decreased.

4. CONCLUSIONS

The numerical analysis of an instrument for hemispherical radiation heat flux measurement, presented in the paper, has shown that it is possible to obtain well defined design parameters under the selection criteria applied. In this respect it was shown:

1. For the selected geometrical parameters of the instrument the required accuracy can be obtained by not exceeding the physical limitation of the material. The range of the working parameters are specified to be $Q_r = 250$–500 kW m^{-2}.
2. Two options of the filament are possible, depending on the range of parameters to be considered. A so-called low efficiency filament and respective blow-off gas mass flow rate is proposed for only radiation heat flux measurements. For working conditions where the convection heat flux has to be considered, a high efficiency filament is proposed.
3. It was proved that under specified working conditions it is possible to obtain a linear relation between the thermal radiation heat flux and the temperature difference between the inlet and outlet blow-off gas, within the range of the thermophysical parameters of the working fluid (air) and of the porous material (stainless steel) and geometrical parameters of the porous filament.

REFERENCES

1. N. H. Afgan and A. I. Leontiev, Instrument for thermal radiation flux measurement in high temperature gas, *Heat Recovery Systems and CHP* (accepted).
2. N. H. Afgan, M. G. Carvalho, N. Martins and A. I. Leontiev, Radiation Heat Flux Instrument. Patent submitted to the Portugal patent authority, 1994.
3. W. Clay and I. S. Davidson, Heat flux-meter in furnace boiler to monitor deposit. *Proc. IMECO Symp. on Thermal and Temperature Measurements in Science and Industry*, Liverpool, 1987, pp. 345–357.
4. E. W. Northover, The CERL Dometer—a radiation heat flux on the tube metal for highly rated boiler. *CEGB Disclosure Bull. No. 294*, 1987.
5. B. Brajuskovic, M. Matovic and N. Afgan, A heat flux-meter for ash deposit monitoring systems—1. Ash deposit prevention. *Int. J. Heat Mass. Transfer* **34(9)**, 2291–2303, 1991.
6. B. Brajuskovic and N. Afgan, A heat flux-meter for ash deposit monitoring systems—"clean" flux-meter characteristics. *Int. J. Heat Mass Transfer* **34(9)**, 2303–2315, 1991.
7. A. I. Leontiev, Heat and mass transfer in turbulent boundary layers. *Advances in Heat Transfer* Vol. 3, pp. 33–100. Academic Press, New York, 1966.
8. M. Kaviany, Principles of heat transfer in porous media. *Mechanical Engineering Series*. Springer, New York, 1991.
9. N. Wakao and S. Kaguei, *Heat and Mass Transfer in Packed Beds*. Gordon and Breach, London, 1982.
10. D. B. Spalding, A novel finite difference formulation for differential expressions involving both first and second derivatives. *Int. J. Numer. Meth. Engng* **4**, 757, 1972.
11. L. S. Caretto *et al.*, Two calculation procedures for steady, three-dimensional flows with recirculation. *Proc. 3rd Int. Conf. Numer. Methods in Fluid Dynamics*. Springer, New York, 1972.